

Hall Effect in spinor condensates

Mathieu Taillefumier¹, Eskil K. Dahl¹, Arne Brataas¹ and Walter Hofstetter²

¹*Department of Physics, Norwegian University of Science and Technology, N-7491 Trondheim, Norway*

²*Institut für Theoretische Physik, J. W. Goethe-Universität Max-von-Laue-Str. 1, 60438 Frankfurt/Main, Germany*

(Dated: November 10, 2018)

We consider a neutral spinor condensate moving in a periodic magnetic field. The spatially dependent magnetic field induces an effective spin dependent Lorentz force which in turn gives rise to a spin dependent Hall effect. Simulations of the Gross-Pitaevskii equation quantify the Hall effect. We discuss possible experimental realizations.

PACS numbers: 03.65.Sq, 03.65.Vf, 03.75.Lm, 03.75.Mn, 03.75.Nt

In 1879, Edwin Hall discovered that charges in a thin metallic plate exposed to a perpendicular magnetic field accumulate transverse to applied electric and magnetic fields. This Hall effect is used intensively to characterize metals and semi-conductors. Modern interest in Hall effects started with the experimental discovery of the quantum Hall effect in two-dimensional electrons gases (2DEG) and the seemingly disconnected notion of Berry curvature [1] and non abelian gauge field [2]. Currently these notions explain the integer and fractional quantum Hall effect in 2DEG, the anomalous Hall effect (AHE) in ferromagnetic metals or semi-conductors and the spin analogue known as spin Hall effect [3].

Three mechanisms contribute to the AHE. Two of them, the side-jump [4] and the skew scattering [5], result from carrier scattering off impurities while the Karplus-Luttinger term [6], also known as Berry curvature contribution, is related to spin-orbit coupling or non trivial magnetic order [7] in the band structure. The latter contribution has attracted considerable theoretical attention although it is very difficult to study experimentally in ferromagnetic compounds because of the additional contributions from impurities or defects.

The realization of Bose-Einstein condensation in magnetic or optical trap opens up the possibility of research at the border between atomic and condensed matter physics. Analogies between condensates in rotating magnetic traps and electrons in strong magnetic fields allow studies of the integer and fractional quantum Hall states [8, 9]. Recently, the realization of spin dependent optical lattices in combination with cold atomic gases [10] offers the possibility to study spin-dependent transport phenomena. The neutrality of these gases, *i.e.* the absence of a classical Lorentz force and the absence of impurity scattering, allows us to study the spin Hall effect [11, 12, 13, 14, 15] and the Berry curvature contribution of the AHE [14] in a clean and controllable environment. So far, the single particle approximation is often used to explain the AHE and SHE in cold atomic gases [11, 13, 14]. Although the single particle approximation can be used to describe qualitatively the AHE in multicomponent condensates, two-body interactions should be included in the theory for a quantitative de-

scription of the Hall effect.

Magnetic microtraps [16] might also be used to study the AHE and SHE in Bose condensates. In this case, the Zeeman effect leads to a coupling between the spin of the atoms and the magnetic field of the microtrap. Various geometries of magnetic field distributions including one-dimensional magnetic lattices have been explored experimentally [16], and two-dimensional magnetic lattices can be created using array of magnetic cylinders [17] or magnetic dots for instance.

In this letter, we investigate the Hall effect in spinor condensates where the magnetic field is created by a two-dimensional array of magnetic cylinders. The motion of the condensate through the magnetic lattice generates a non abelian gauge field that acts on the condensate as an effective spin dependent Lorentz force [18]. Similarly to the case of fermions [19], we first study the case where the two-body interactions are negligible. Then we study numerically the effect of the velocity of the condensate and of the non linear interactions on the Hall Effect. Finally we propose an experimental setup where this effect can be observed.

Let us consider a quasi-two-dimensional spinor condensate of spin F moving in a magnetic field $\mathbf{B}(\mathbf{r})$ created by a 2D array of magnetic cylinders. The Hamiltonian describing this system is [20, 21, 22]

$$\mathcal{H} = \int d^2\mathbf{r} \psi_\alpha^\dagger(\mathbf{r}) \left(\left[-\frac{\hbar^2}{2M} \nabla_{\mathbf{r}}^2 + V(\mathbf{r}) \right] \delta_{\alpha\delta} + (\mathbf{B}(\mathbf{r}) \cdot \mathbf{F})_{\alpha\delta} \right. \\ \left. + \sum_{s=0}^F \frac{\sqrt{2\pi}\hbar^2 a_{2s}}{M a_z} (\mathcal{P}^{2s})_{\alpha\beta\gamma\delta} \psi_\beta^\dagger(\mathbf{r}) \psi_\gamma(\mathbf{r}) \right) \psi_\delta(\mathbf{r}) \quad (1)$$

where $\psi_\alpha(\mathbf{r})$ with $\alpha = -F, \dots, F$ are the spin components of the quantum field operator $\Psi(\mathbf{r})$, and \mathcal{P}^{2s} is the projection operator that projects the spin state of the atoms pair into the total spin state $2s$. $F^{l=x,y,z}$ are matrices of spin F and the constants a_{2s} are the s-wave scattering lengths of the total spin channel $2s = 0, 2, \dots, 2F$. The confinement in the z direction appears in the Hamiltonian via the oscillator length $a_z = \sqrt{\hbar/M\omega_z}$, $\omega_z = 2\pi f_z$ where f_z is the frequency of the trap along the z direction and M the mass of the atoms. The scalar potential $V(\mathbf{r})$ describes any external trap potential. Following

Ref. [19], we apply a rotation $\mathcal{T}(\mathbf{r})$ of the quantization axis along the direction $\mathbf{n}(\mathbf{r})$ of the magnetic field $\mathbf{B}(\mathbf{r})$ to (1). The transformed Hamiltonian becomes

$$\begin{aligned} \mathcal{H}_{\mathcal{T}} = & \int d^2\mathbf{r} \psi_{\alpha}^{\dagger}(\mathbf{r}) \left[\left[-\frac{\hbar^2}{2M} (\nabla_{\mathbf{r}} - i\mathbf{A}_g(\mathbf{r}))^2 + V(\mathbf{r})\delta_{\alpha\gamma} \right] \right. \\ & + |\mathbf{B}(\mathbf{r})| F_z^{\alpha\delta} \\ & \left. + \sum_{s=0}^F \frac{\sqrt{2\pi}\hbar^2 a_{2s}}{M a_z} (\mathcal{P}^{2s})_{\alpha\beta\gamma\delta} \psi_{\beta}^{\dagger}(\mathbf{r}) \psi_{\gamma}(\mathbf{r}) \right] \psi_{\delta}(\mathbf{r}), \quad (2) \end{aligned}$$

where $\mathbf{A}_g(\mathbf{r}) = -i\mathcal{T}^{\dagger}(\mathbf{r})\nabla_{\mathbf{r}}\mathcal{T}(\mathbf{r}) = \mathbf{A}_g^i(\mathbf{r})F^i$ with $i = x, y, z$ is the spin dependent gauge field resulting from the rotation of the spin axis. Explicit expressions for $\mathbf{A}_g^i(\mathbf{r})$ ($i = x, y, z$) can be found in Ref. [23]. The two-body interactions are not affected by the gauge transformation because they are short ranged and the projection operators are invariant against any rotation of the spin axis of both particles. Excluding the two-body interactions, Eq. (2) is a generalization of Eq. (2) of Ref. [19] for both fermions and bosons. The present work has two additional ingredients, the non linear interactions and the relaxation of the adiabaticity condition. The non abelian gauge field $\mathbf{A}_g(\mathbf{r})$ contains terms that are proportional to F^x and F^y that induce transitions between the different spin-polarized states.

Approximate analytical calculations: Let us initially assume that the spin-flip transitions can be neglected, *i.e.*, that the spin adiabatically follows the magnetic field direction $\mathbf{n}(\mathbf{r})$. This approximation will be lifted later on. In contrast to $F = 1/2$, the expansion of Eq. (2) gives rise to two spin-flip terms that are proportional to $\mathbf{A}_g(\mathbf{r})$ and $\mathbf{A}_g(\mathbf{r}) \cdot \mathbf{A}_g(\mathbf{r})$. The adiabatic approximation is valid when $\nu_1 = \frac{\hbar v}{2\xi\Delta_z} \ll 1$ and $\nu_2 = \frac{\hbar^2}{2m\xi^2\Delta_z} \ll 1$ are fulfilled. The constant v is the group velocity of the particles, ξ is a characteristic length of variations of $\mathbf{n}(\mathbf{r})$ and Δ_z is the Zeeman splitting. The two-body interactions are included in Eq. 2 through a spin-spin interaction term that can be decomposed into a scalar and a spin-dependent contribution [21]. The typical energy scale of the scalar inter-atomic interaction component is of the order of magnitude of the Zeeman splitting. The spin-dependent part of the two-body interactions, on the other hand, can be neglected because it is two to three orders of magnitude smaller than the scalar contribution. For this semi-classical analysis, we neglect the two-body interactions and assume that the spinor condensate is in a spin polarized state $m \in [-F, \dots, F]$. The effective Hamiltonian can be written as

$$\begin{aligned} \mathcal{H}_{\text{eff}} = & \int d^3\mathbf{r} \psi_m^{\dagger}(\mathbf{r}) \left[\frac{\hbar^2}{2M} (-i\nabla_{\mathbf{r}} + m\mathbf{A}_g^z(\mathbf{r}))^2 + V(\mathbf{r}) \right. \\ & \left. + m|\mathbf{B}(\mathbf{r})| \right] \psi_m(\mathbf{r}). \quad (3) \end{aligned}$$

There is a difference between bosons and fermions. For fermions, all spin polarized states are affected by the

gauge field $\mathbf{A}_g^z(\mathbf{r})$ while for bosons, the spin polarized state $m = 0$ is not affected by the magnetic texture. So for $m \neq 0$ the field $\mathbf{b}_g(\mathbf{r}) = \nabla \times \mathbf{A}_g^z(\mathbf{r}) = \varepsilon_{ijk} n_i \partial_x n_j \partial_y n_k$ acts on the spin polarized state as an ordinary magnetic field on a fictitious charge $q = me$ ($-e$ is the electron charge), and then gives rise to an effective Lorentz force [18] that can induce a Hall effect.

For a qualitative analysis, we consider the case where the average value of the field $\langle \mathbf{b}_g(\mathbf{r}) \rangle_s$ over one unit cell acts on the dynamics of the condensate. Firstly, the average value $\langle \mathbf{b}_g(\mathbf{r}) \rangle_s = 4\pi n/S$ with ($n \in \mathbb{Z}$) and S the surface of the unit cell, is quantized and depends only on few geometrical parameters such as the type and the period of the lattice. This value can be modified by applying a small constant magnetic field on top of the magnetic distribution [19]. Secondly, the spatial dependence of the field $\mathbf{b}_g(\mathbf{r})$ and the potential $|\mathbf{B}(\mathbf{r})|$ are treated phenomenologically as causing momentum scattering that is characterized by the relaxation time τ . We consider moreover that the condensate is under the influence of a force $\mathbf{F} = F_0\mathbf{x}$ where F_0 is the amplitude. Such forces can be induced by gravity for instance. The dynamics of the center of mass of the spin polarized state is described by:

$$M \frac{d\langle \mathbf{v} \rangle}{dt} = F_0\mathbf{x} - m \left(\frac{\langle \mathbf{v} \rangle}{\tau} + \hbar \langle \mathbf{v} \rangle \times \langle \mathbf{b}_g \rangle_s \right), \quad (4)$$

where $\langle \mathbf{v} \rangle$ is the center-of-mass velocity of the polarized state. The solutions of Eq. (4) are simple and the wave packet trajectories go from closed orbits when there is no scattering and no force to open orbits when scattering and/or external force are present. One can also show that the quantity $\sigma_{xy} = \langle v_y \rangle / F_0$ is similar to the Drude formula of the Hall conductivity component. The Hall effect is stronger when the spin F increases or the surface of the unit cell decreases.

Numerical simulations: A quantitative study of the Hall effect in this systems can be done by solving Eq. (1) numerically using mean field theory. The order parameters of the spinor condensate, which are the expectation values of the field operators $\psi_{\alpha}(\mathbf{r})$, obey the time dependent Gross-Pitaevskii equation (TDGP) obtained from Eq. (1) by substituting $\psi_{\alpha}(\mathbf{r})$ by its average. We solve the TDGP equation using an explicit Runge-Kutta method of order six coupled to the Fast Fourier transform for the spatial derivatives. For the magnetic field distribution, we consider a square lattice of magnetic cylinders.

The initial state of the system is obtained in the following way. We first calculate the ground state of a spinor condensate of spin $F = 1$ composed of 2000 atoms of rubidium [24] in an harmonic trap with $\omega_x = \omega_y = 2\pi \times 50$ Hz ($\omega_z = 2\pi \times 1000$ Hz). Then the condensate is shifted to one side of the trap and the wave-function is multiplied by a phase factor $\exp(ivx)$ where v is the group velocity. At $t = 0$ the condensate is released from

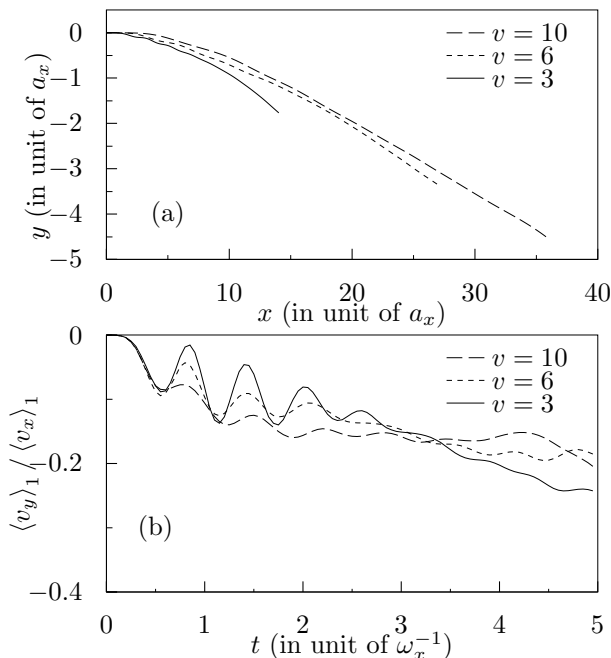


FIG. 1: (a) Transverse position as a function of longitudinal coordinate of the center of mass of a $F = 1$ condensate for $t\omega_x \leq 5$ and different values of the initial group velocity v (in units of $a_x\omega_x$). (b) Time dependence of the ratio of average transverse and longitudinal velocity. The initial state is prepared in the ferromagnetic state $m = 1$.

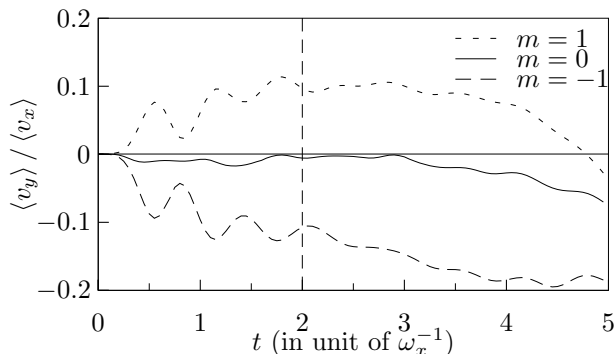


FIG. 2: Time dependence of the ratio $\langle v_y \rangle / \langle v_x \rangle$ calculated for different initial polarizations and fixed initial velocity $v = 6$. The vertical lines indicates the separation between the adiabatic regime where spin flip contributions are negligible from the regime where they dominate the dynamics of the condensate.

the harmonic trap and is able to move freely through the magnetic lattice.

To characterize the Hall effect, we calculate the ratio between the transverse and longitudinal velocity

$$\langle v_y \rangle_m / \langle v_x \rangle_m = \sigma_{xy} / \sigma_{xx}, \quad (5)$$

where m indicates the initial polarization of the condensate at $t = 0$ (in the global quantization axis which is along the z axis) and $\langle v_{i=x,y} \rangle_m$ is the average value of the

velocity operator. σ_{xy} and σ_{xx} are the transverse and longitudinal "conductivities". This ratio corresponds physically to the tangential of the angle between the electrical field and the velocity in the case of electronic systems. For convenience, we express all quantities in reduced units $x \rightarrow a_x x$ with $a_x = \sqrt{\frac{\hbar}{M\omega_x}} \approx 1.59 \mu\text{m}$ and the energy $\varepsilon \rightarrow \varepsilon \hbar \omega_x$. Finally we choose the following set of parameters of the magnetic field. The period of $\mathbf{B}(\mathbf{r})$ is $p = 7.5 a_x$, the amplitude is $B = 10 \hbar \omega_x$ and the distance separating the condensate from the surface of the magnetic array is $h = 1.5 a_x$.

The dynamical behavior of the TDGP equation is visualized in Fig. 1 which represents the ballistic trajectory of the center-of-mass of the Bose condensate (fig. 1-a) and the Hall angle (fig. 1-b) for different values of the initial velocity. Fig. 1-a shows that the trajectory of the condensate prepared in the state $m = 1$ is curved in the y direction because of the action of the gauge field on the dynamics of the condensate as qualitatively described by Eq. 3. Fig. 1-b represents the time dependence of the ratio $\langle v_y \rangle_{m=1} / \langle v_x \rangle_{m=1}$. It shows pronounced oscillations at early stages of the evolution that can be understood qualitatively by considering the sign of the effective Lorentz force that is acting on the condensate. Since the size of the condensate is smaller than the size of the unit cell, part of the condensate will experience a positive Lorentz force while its complementary part will experience a negative Lorentz force. Due to the distribution of particles in the condensate and the different topology of the regions where the field $\mathbf{b}_g(\mathbf{r})$ is positive or negative, the Lorentz force changes sign when the condensate is moving through the lattice and the y component of the group velocity oscillates with time. The oscillations of $\langle v_y \rangle_{m=1} / \langle v_x \rangle_{m=1}$ quickly disappear when t increases because (i) the condensate expands and (ii) the magnetization is not conserved so the mean field state describing the condensate tends to a state with equipartition in populations ($n_{\pm 1,0} = 1/3$). Numerical simulations show that these oscillations remain when the size of the unit cell is smaller than the size of the condensate, as it should be expected.

The dynamical properties of the system can be separated into two different regimes; the adiabatic regime where the spin polarized state follows adiabatically $\mathbf{B}(\mathbf{r})$ as described by our approximate analytical calculations and a second regime that is dominated by the spin flip terms. The adiabatic regime can be identified at early time of the evolution of the condensate by calculating the ratio $\langle v_y \rangle / \langle v_x \rangle$ for the spin polarized states $m = 1$ and $m = -1$. In this case, Eq. (3) shows that the two angles should differ by a sign which can be seen on the left part of Fig. 2. This behavior is not peculiar to Bose condensates and should be observable with fermionic atomic gases or electrons gases provided that the gas is initially fully polarized and there is no disorder. As expected from

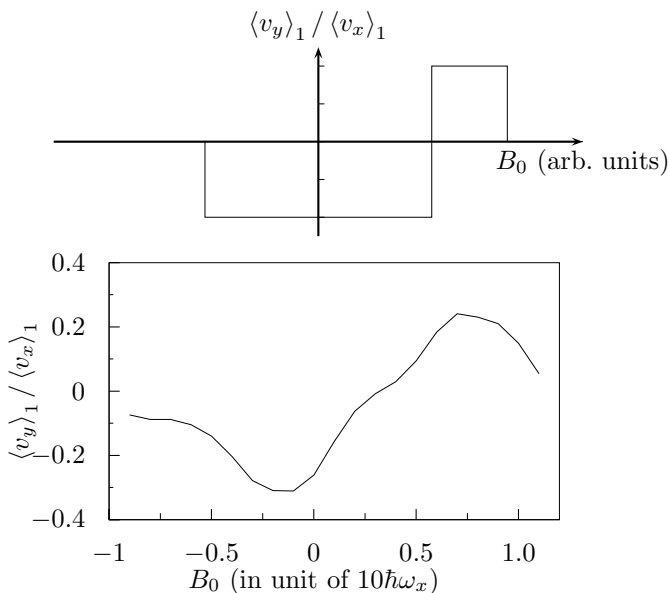


FIG. 3: (upper panel) schematic dependence of the Hall conductivity when a constant magnetic field is applied on the top of the magnetic lattice. The abrupt changes in $\langle v_y \rangle_1 / \langle v_x \rangle_1$ are related to the flux of $\mathbf{b}_g(\mathbf{r})$ which changes sign at a peculiar value of B_0 . (lower panel) numerical results for the ratio $\langle v_y \rangle_1 / \langle v_x \rangle_1$ ($5\omega_x^{-1}$) as a function of the magnetic field amplitude.

Eq. (3), there should be no Hall effect for the polar state ($m = 0$) which can also be observed in Fig. 2. Fig. 2 shows that $\langle v_y \rangle_0 / \langle v_x \rangle_0$ of an initial polar state fluctuates around zero. These fluctuations are not affected by the spin-dependent part of the two-body interactions but are related to the spin-flip contributions of the gauge field $\mathbf{A}_g(\mathbf{r})$. At longer time (right part Fig.2), the dynamics of the condensate is governed by the spin-flip terms and the description of the Hall effect in terms of the adiabatic approximation in (3) is not valid anymore.

Finally, we study the influence of a small constant magnetic field of amplitude B_0 applied on top of the magnetic lattice in the direction perpendicular to the plane of motion. Contrary to Ref. [19] which consider the electronic case, there is no classical Hall effect because the atoms are neutral. Therefore the features of the anomalous Hall effect are easily observed in Bose condensates. In the semiclassical limit, *i.e.* when the spatial dependence of the gauge field is neglected, the variations of the Hall angle are abrupt because the average value of $\mathbf{b}_g(\mathbf{r})$ can only change at peculiar values of B_0 which depends on the lattice. Such variations are schematically represented on the upper panel of Fig.3. The general behavior described in the upper panel of Fig.3 can be reproduced numerically using the full time-dependent GP equation but the variations of the ratio $\langle v_y \rangle / \langle v_x \rangle$ are continuous rather than abrupt (lower panel of Fig.3). The numerical simulations also show that the Hall effect decrease rapidly when the

amplitude of the constant magnetic field increases.

To experimentally verify this theory, we propose to image the motion of a spin polarized condensate during its evolution in a microtrap with an additional periodic 2d magnetic field and deduce the ratio $\langle v_y \rangle / \langle v_x \rangle$ by direct measurement of the velocity. The magnetic lattice can be created using arrays of magnetic cylinders or by patterning lattices of interconnected current loops. The condensate can be accelerated through gravity by tilting the microtrap.

To conclude, we have shown that spinor condensates in a magnetic lattice can be used to explore the geometrical phase contribution of the anomalous Hall effect. We found that this contribution is characterized by an adiabatic regime which is valid in the short time limit and a long time regime where spin-flip processes dominate the condensate dynamics. We also demonstrated that the AHE is strongly affected by an additional constant external magnetic field.

The authors thank M. Snoek, B. Canals, C. Lacroix, V. Dugaev, P. Bruno and J. Dalibard for discussion. This work was supported in part by Forschergruppe FOR 801 of the Deutsche Forschungsgemeinschaft.

-
- [1] M. V. Berry, Proc. R. Soc. **392**, 45 (1984).
 - [2] F. Wilczek and A. Zee, Phys. Rev. Lett. **52**, 2111 (1984).
 - [3] J. Sinova *et al.*, Phys. Rev. Lett. **92**, 126603 (2004).
 - [4] L. Berger, Phys. Rev. B **2**, 4559 (1970).
 - [5] J. Smit, physica (Amsterdam) **21**, 877 (1955), physica (Amsterdam) **24**, 39 (1958).
 - [6] R. Karplus and J. Luttinger, Phys. Rev. **95**, 1154 (1954).
 - [7] S. Onoda and N. Nagaosa, Phys. Rev. Lett. **90**, 196602 (2003).
 - [8] R. Bhat, *et al*, Phys. Rev. A **76**, 043601 (2007).
 - [9] S. Viefers, J. Phys. Condensed matters **20**, 123202 (2008).
 - [10] O. Mandel, *et al*, Phys. Rev. Lett. **91**, 010407 (2003).
 - [11] X.-J. Liu, *et al*, Phys. Rev. Lett. **98**, 026602 (2007).
 - [12] K. Y. Bliokh and Y. P. Bliokh, Phys. Rev. Lett. **96**, 073903 (2006).
 - [13] S.-L. Zhu, *et al*, Phys. Rev. Lett. **97**, 240401 (2006).
 - [14] A. M. Dudarev, *et al*, Phys. Rev. Lett. **92**, 153005 (2004).
 - [15] J. Ruseckas, *et al*, Phys. Rev. Lett. **95**, 010404 (2005).
 - [16] J. Fortágh and C. Zimmermann, Rev. Mod. Phys. **79**, 235 (2007).
 - [17] K. Nielsch *et al*, Appl. Phys. Lett. **79**, 1360 (2001)
 - [18] Y. Aharonov and A. Stern, Phys. Rev. Lett. **69**, 3593 (1992).
 - [19] P. Bruno, *et al*, Phys. Rev. Lett. **93**, 96806 (2004).
 - [20] T. Ohmi and K. Machida, J. Phys. Soc. Jpn. **67**, 1822 (1998).
 - [21] T.-L. Ho, Phys. Rev. Lett. **81**, 742 (1998).
 - [22] Y. Castin and R. Dum, Eur. Phys. j. D **7**, 399 (1999).
 - [23] A. Bohm, *et al*, *The Geometric Phase In quantum systems* (Springer, 2003), iSSN 0172-5998.
 - [24] The s-wave scattering lengths for Rubidium are $a_0 = 101.8 a_B$ and $a_2 = 100.4 a_B$ where a_B is the Bohr

radius[25]. (2002).
[25] E. van Kempen *et al.*, Phys. Rev. Lett. **88**, 093201